

RELATIVE DECAY RATE DETERMINATION

A RELATIVE METHOD FOR DETERMINATION
OF
NUCLEAR DECAY RATES

By

DONALD D. BURGESS, B. Sc.

A Thesis

Submitted to the School of Graduate Studies
in Partial Fulfilment of the Requirements

for the Degree

Master of Science

McMaster University

July, 1974

MASTER OF SCIENCE (1974)
(Chemistry)

McMASTER UNIVERSITY
Hamilton, Ontario

TITLE: A Relative Method for Determination
of Nuclear Decay Rates

AUTHOR: Donald D. Burgess, B.Sc. University of Waterloo

SUPERVISORS: Dr. T.J. Kennett
Dr. K. Fritze

NUMBER OF PAGES: vi 63

ABSTRACT

The performance of a relative decay rate measurement technique was investigated. Determinations of the half-lives of the isotopes copper-64 and ruthenium-97 in various chemical states were attempted as illustrations of the use of the method. Applications of the technique are suggested.

ACKNOWLEDGEMENTS

I wish to express my sincere gratitude to my supervisors Dr. T.J. Kennett and Dr. K. Fritze for their kind help in this work. Particular thanks are due to Dr. T.J. Kennett and Mr A. Robertson for their help with statistical problems and with the equipment and to Mr J. Skene for his help in computer programming. I also wish to thank my mother for her patient typing of the manuscript.

TABLE OF CONTENTS

		Page
Chapter I	INTRODUCTION	1
	Half-life Perturbation	5
Chapter II	EXPERIMENTAL PROCEDURES	8
	Chemical Preparations	8
	Activity Measurements	10
	Data Reduction	11
Chapter III	RESULTS	13
Chapter IV	DISCUSSION	17
Chapter V	CONCLUSION	22
Appendix A	ELECTRON CAPTURE DECAY	23
Appendix B	OPTICAL SPECTRUM OF RuO₄.py2	25
Appendix C	COMPUTER PROGRAM FOR SPECTRUM ANALYSIS	27
Appendix D	DERIVATION OF UNCERTAINTY FORMULAE	60
Bibliography		62

LIST OF ILLUSTRATIONS

Figure		Page
1	Decay Schemes for Cu ⁶⁴ and Ru ⁹⁷	6
2	Copper and Potassium Gamma Ray Spectrum	15
3	Ruthenium and Gold Gamma Ray Spectrum	16
4	Ruthenium and Gold: ln (A ₁ /A ₂) vs Time	19
5	Optical Spectrum of RuO ₄ , py2	26
6a	Flowchart for Program 1	28
6b	Flowchart for Program 2	29
6c	Flowchart for Subroutine Plt	30
6d	Flowchart for Subroutine Plt	31
6e	Flowchart for Program 3	32

LIST OF TABLES

Table		Page
I	Half-lives of Reference Isotopes	7
II	Gamma Radiation Energies	12
III	Half-life Results	13

INTRODUCTION

The use of lithium drifted germanium (Ge (Li)) detectors for the measurement of nuclear gamma radiation has increased dramatically in recent years. When used in conjunction with a multichannel pulse-height analyzer, these detectors provide a convenient method of obtaining gamma ray spectra. The energy scale of such spectra is easily calibrated by means of standard isotopes which radiate at known energies.

The determination of the absolute or relative intensity of a line in a spectrum collected with a Ge (Li) detector is, unfortunately, not as straight forward. The difficulties encountered in these measurements also complicate the use of Ge (Li) spectra for half-life determinations since intensity variation with time is the information required.

The quantities commonly found from a spectrum are the position of peaks and the areas below them. The position of a peak depends upon the energy of the detected radiation. The area below a peak depends not only upon the intensity of the radiation received, but also upon several other effects.

The more important factors contributing to peak area are; detector efficiency, background radiation, Compton scattering, and count-rate dependent effects such as electronic

dead time and pulse pile-up. All of these effects must be accommodated before meaningful half-life data can be obtained from Ge (Li) spectra.

Despite the difficulties mentioned above, the use of Ge (Li) detectors for half-life studies is desirable. Their good energy resolution permits the use of sources which are not radiochemically pure. Except in unfavourable circumstances, each peak in the spectrum can be considered separately, and those due to impurities can be ignored. Counting devices, such as ionization chambers, which lack this energy resolution, do not permit this latitude.

The method of half-life measurement presented here is a relative one. The isotope of interest is counted with a reference isotope of known half-life. Ge (Li) spectra are obtained over a period of time, and peak areas due to sample and reference isotopes are found. The mathematical basis of the method follows.

Consider two isotopes a and b having decay constants λ_a and λ_b , and activities A_a and A_b . The decay law gives the following:

$$\frac{A_a}{A_b} = \frac{A_a^0}{A_b^0} \cdot \frac{e^{-\lambda_a t}}{e^{-\lambda_b t}} = \frac{A_a^0}{A_b^0} e^{(\lambda_b - \lambda_a)t}$$

where t is time and A_a^0 and A_b^0 are activities at $t=0$. Note that $\frac{A_a^0}{A_b^0}$ is a constant.

Rearranging, and taking the natural logarithm gives

$$(\lambda_b - \lambda_a)t = \ln\left(\frac{A_a}{A_b}\right) + \ln\left(\frac{A_a^0}{A_b^0}\right)$$

and taking the derivative with respect to t gives

$$(\lambda_b - \lambda_a) = \frac{d}{dt} \left(\ln \left(\frac{A_a}{A_b} \right) \right) + 0$$

In graphical terms, the slope of $\ln \left(\frac{A_a}{A_b} \right)$ versus time is the difference in decay constants λ_a and λ_b .

Call $(\lambda_b - \lambda_a) = \Delta \lambda_{ab} \quad \therefore \lambda_a = \lambda_b - \Delta \lambda_{ab}$

From this, $t_{1/2}^a = \frac{0.693}{\lambda_b - \Delta \lambda_{ab}}$

where $t_{1/2}^a$ is the half-life of isotope a .

Therefore, if the ratio of sample - to standard - isotope activity is followed in time, the half-life of the sample isotope can be found. If the counting time is much less than the isotope half-life, peak area is proportional to activity.

The contributions to peak area, other than the radiation intensity, can be overcome by this technique. A detector's efficiency depends mainly on two considerations; the material of which it is constructed, and the source - detector geometry. If the source - detector geometry is carefully maintained the same, it can be assumed that the collection efficiency will remain unchanged.

The effects of background radiation and Compton scattering result in a "level" in the spectrum upon which the peak appears. This is usually dealt with during determination of peak areas.

The corrections for system dead time and, to some

extent, for pulse pile-up are accomplished automatically. System dead time refers to the fact that a multichannel analyzer requires a period of time to process a signal due to a detected event. During this time, other signals are lost. The fraction of counts lost depends on the count rate, and, therefore, on time since the count rate decreases as the source decays. However, unless the intensities are very different, the fraction of counts lost is the same for all peaks in the spectrum. The ratio of peak areas is therefore unchanged.

At very high count rates, pulse pile-up may occur. This happens when a pulse occurs in the detection system sufficiently soon after a preceding one to combine their heights. Instead of two pulses, the system registers one pulse with an energy somewhere between the individual components and their sum. The effect is to remove counts from the peaks and to change the shape of the spectrum.

However, all peaks in the spectrum are affected in the same way, (Anders 69) and the ratios of peak-areas are unaffected by pulse pile-up.

This relative method of measuring half-lives, therefore, avoids the problems of estimating losses due to dead-time and pulse pile-up which trouble other methods.

Half-life Perturbation

It has been found that the decay constants for electron-capture and internal conversion processes are subject to minute changes when the physical or chemical environment of the decaying nucleus is changed. The electron-capture mode of decay was chosen for study by the half-life measurement technique described above. Previous work on half-life changes has been done using balanced ionization chambers (Bainbridge 53), paired sodium iodide detectors (Gagneux 70) and magnetic deflection instruments.

In his review paper on this subject, G.T. Emery (Emery 72) reaches the conclusion that perturbations of decay rates in electron capture are mainly dependent upon changes in electron density at the nucleus. A discussion of electron capture can be found in Appendix A. Changes in chemical state can be expected to affect this electron density, and, therefore, the decay rate of the nucleus.

The isotopes chosen for study were copper-64 and ruthenium-97. Their decay schemes are given in Figure 1. The decay constant of copper-64 has been reported to change by as much as a percent (Kemany 68). However, later work (Wyatt 72) has failed to confirm this. For copper, the metal was compared with the formally doubly ionized solution species. The metal was compared with the formally eight-positive state for ruthenium.

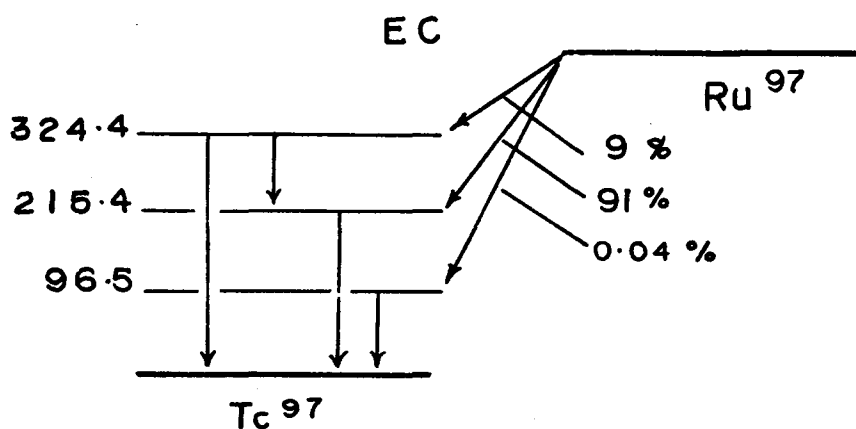
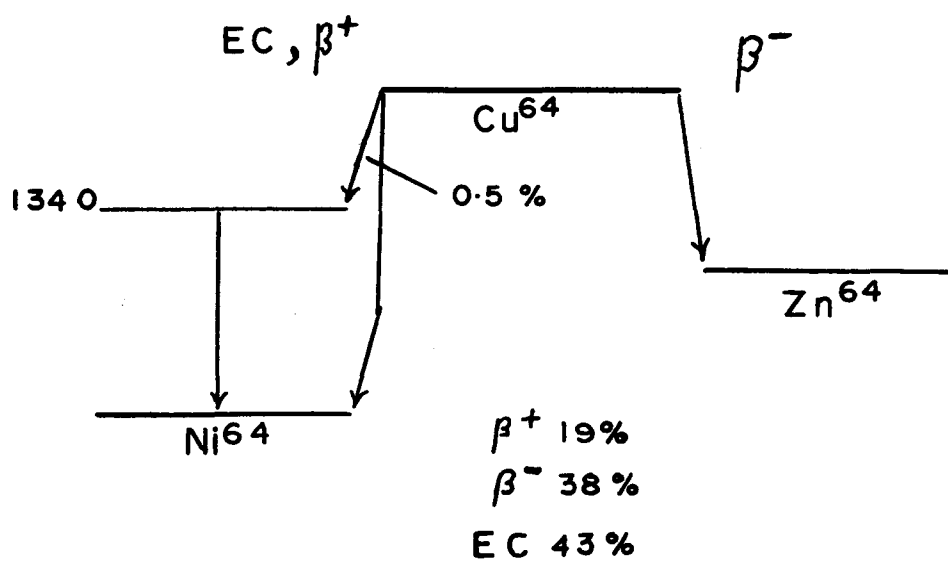


Figure 1

Decay Schemes

Potassium-42 was used as the reference isotope for measurements on copper, and gold-198 was used as the reference for ruthenium. The reported half-life data for these isotopes is given in Table I.

Table I

Half-Lives for Reference Isotopes

<u>Isotope</u>	<u>Half-life</u>	<u>Reference</u>
K ⁴²	12.358 ± 0.003 hr	Merritt 62
Au ¹⁹⁸	2.6946 ± 0.0010 d	Cabell 70

The difference in half-life between two sample sources can be calculated from the differences $\Delta\lambda_i$, measured and the half-life of the reference isotope as follows: for sample isotopes a and b and reference isotope r,

$$\Delta\lambda_{ar} = \lambda_r - \lambda_a$$

$$\Delta\lambda_{br} = \lambda_r - \lambda_b$$

$$\lambda_a - \lambda_b = \Delta\lambda_{br} - \Delta\lambda_{ar}$$

that is, $\Delta\lambda_{ba} = \Delta\lambda_{br} - \Delta\lambda_{ar}$

Changes in decay constant are customarily reported as

$$\frac{\Delta\lambda_{ba}}{\lambda_b} . \quad \frac{\Delta\lambda_{ba}}{\lambda_b} = \frac{\Delta\lambda_{br} - \Delta\lambda_{ar}}{\lambda_r - \Delta\lambda_{br}}$$

The result can be converted to half-life units in the usual manner.

EXPERIMENTAL PROCEDURES

Chemical Preparations

Copper Metal

Cupric sulphate powder was irradiated at the McMaster nuclear reactor. It was then dissolved in a solution of sulphuric and nitric acids in distilled water. Copper metal was electroplated from this solution onto a clean copper gauze. Inactive copper was plated onto the gauze before and after deposition of the activated metal. The gauze was washed with distilled water and acetone, air dried, then mounted for counting. Discolouration was not observed.

Aqueous Copper Sulphate

Irradiated cupric sulphate was dissolved in distilled water. Cupric hydroxide was precipitated by addition of aqueous sodium hydroxide and then filtered. The precipitate was then dissolved in dilute sulphuric acid. Active potassium was added in the form of irradiated potassium carbonate. Finally, the solution was placed in a lucite cell for counting. No discolouration of the solution, or formation of precipitate was observed.

Ruthenium Metal

Ruthenium metal was sealed into a quartz ampoule and

irradiated. The ampoule was then cleaned and mounted for counting. The separated isotope Ru⁹⁶ (ORNL Oak Ridge, Tennessee) was used for all ruthenium irradiations.

Ruthenium Tetroxide

The method of Ruff and Vidic (Ruff 24) was used to prepare an aqueous solution of ruthenium tetroxide from a mixture of irradiated ruthenium metal and inactive natural ruthenium. The golden yellow tetroxide was then extracted into cold carbon tetrachloride. It was found that this solution gradually decomposed to give a black solid. Thereafter, the ruthenium tetroxide was prepared as the pyridine complex after Koda (Koda 63). The solid complex was mounted for counting. See appendix B for optical spectrum.

Potassium Carbonate

Potassium carbonate was irradiated in polyethylene vials and was mounted for counting without purification.

Gold oxide

Gold oxide powder was sealed into quartz ampoules for irradiation and counting.

The cupric sulphate used was obtained from Fischer Scientific Co. Potassium carbonate was supplied by the McArthur Chemical Corp. Natural ruthenium metal and gold oxide were supplied by Alpha Inorganics Ltd. All were used

as received.

Activity Measurements

The activity of samples was measured by means of either a lithium drifted germanium detector made in this laboratory or a Harshaw Chemical Co. detector of the same type. A Nuclear Data 160-M multichannel analyzer was used in conjunction with a Digital Equipment Corp. PDP-15 computer for acquisition of spectra.

The samples were fixed by means of tape to lucite holders (or placed in lucite cells if liquid) and placed in a lucite stand for counting. Care was taken to obtain reproducible geometry.

The position of the sample holder was adjusted at the start of each run to give a satisfactory count rate by setting the holder at the required distance from the detector. Each counting period was started and stopped manually. The duration of each period was kept constant for each sample throughout its series of measurements. Several samples were processed during each run.

Data Reduction

Analysis of spectra was carried out by means of an interactive program written for the PDP-15 computer. The data were displayed on a CRT and sections of background on each side of the peak being examined, were chosen by inspection. A straight line was fitted to each section and displayed with the data. Peak boundaries were estimated by selecting the channels at which the fitted lines and peak edges met.

A further straight line was generated between the peak boundaries using data from the previous lines. This was considered to represent the contribution from background to the peak. This assumption is customary in dealing with Ge (Li) spectra (Hoste 71 page 36).

The channels between the peak boundaries were summed, subtracting the value of the background at each channel. The peak area was then printed with an estimate of its uncertainty based on counting statistics. A detailed description of this program may be found in Appendix C.

The ratios of the areas of the appropriate peaks and their natural logarithms were found and plotted against the time at which counting was done. A straight line least squares fit was then conducted.

In one case, two data points were rejected according to Chauvenet's Criterion. This resulted in the reduced chi-square changing to 1.2 from 7.2 and the slope from 0.00056

to 0.00046. The final slope agrees with that obtained from a sample run concurrently.

A sample of the long-lived isotope cobalt-60 was counted several times under the same conditions as for the samples investigated in this study. The natural logarithm of the ratio of the peak areas for the lines at 1173Kev and 1332 Kev were found in each case. This quantity should be the same within statistical variations for each count. As this was not found, the standard deviation of these data was found and was used as an estimate of the uncertainty in the data of all measurements made. The calculation followed that given by Bevington (Bevington 69).

For the analysis of spectra, the following radiations were used:

Table II
Gamma Radiation Energies

<u>Isotope</u>	<u>γ-energy (Kev)</u>
K ⁴²	1524
Cu ⁶⁴	511 (annh.)
Au ¹⁹⁸	412
Ru ⁹⁷	215

RESULTS

Typical spectra for the copper and ruthenium measurements are shown in figures 2 and 3.

Repeated measurements with cobalt-60 yielded a standard deviation of 6.19% for the quantity $\ln\left(\frac{A_a}{A_b}\right)$. The average standard deviation predicted from counting statistics was subtracted in quadrature, and the residue was added to the counting statistics predicted for each measurement in similar fashion.

The half-life measurements made gave the results shown in Table III

Table III

Half-life Results

<u>Isotope</u>	<u>State</u>	<u>Half-life</u>
Cu ⁶⁴	metal	12.947 ± 0.077 hr
		12.702 ± 0.078 hr
		12.566 ± 0.048 hr
	solution	$12.652 \quad 0.061$ hr
		$12.818 \quad 0.051$ hr
		$12.743 \quad 0.071$ hr
Ru ⁹⁷	metal	2.7654 ± 0.0052 d
		2.8156 ± 0.0080 d
		2.8599 ± 0.0083 d

<u>Isotope</u>	<u>State</u>	<u>Half-life</u>
	oxide	2.7922 \pm 0.0049 d
		2.8167 \pm 0.0096 d
		2.8382 \pm 0.0106 d

Six trials using active copper and potassium yielded a mean of 12.71 ± 0.14 hr as the half-life of copper-64. No difference in half-life was observed in comparing the metal and dissolved forms. The uncertainty in this measurement was $\pm 1.7\%$ expressed as $\frac{\Delta\lambda}{\lambda}$. The literature gives a value of 12.71 ± 0.01 hr for the half-life of copper-64 (Wyatt 72) which is in good agreement with the present result.

As table 3 shows, the results of the ruthenium experiments were not reproduceable. The spectra from each run were further investigated. It was concluded (see discussion section) that the two runs which yielded lower half-life values may have been subject to instrumental interference. The run which yielded a mean value of 2.8497 ± 0.0065 d was apparently free of these effects. However, these data were insufficient to draw conclusions about possible half-life changes.

Literature values for the half-life of ruthenium-97 vary widely. However, the value 2.88 d given by Katcoff (Katcoff 58) appears to be favoured (Lederer 67) although no uncertainty is given. The half-life found is in only rough agreement with this determination.

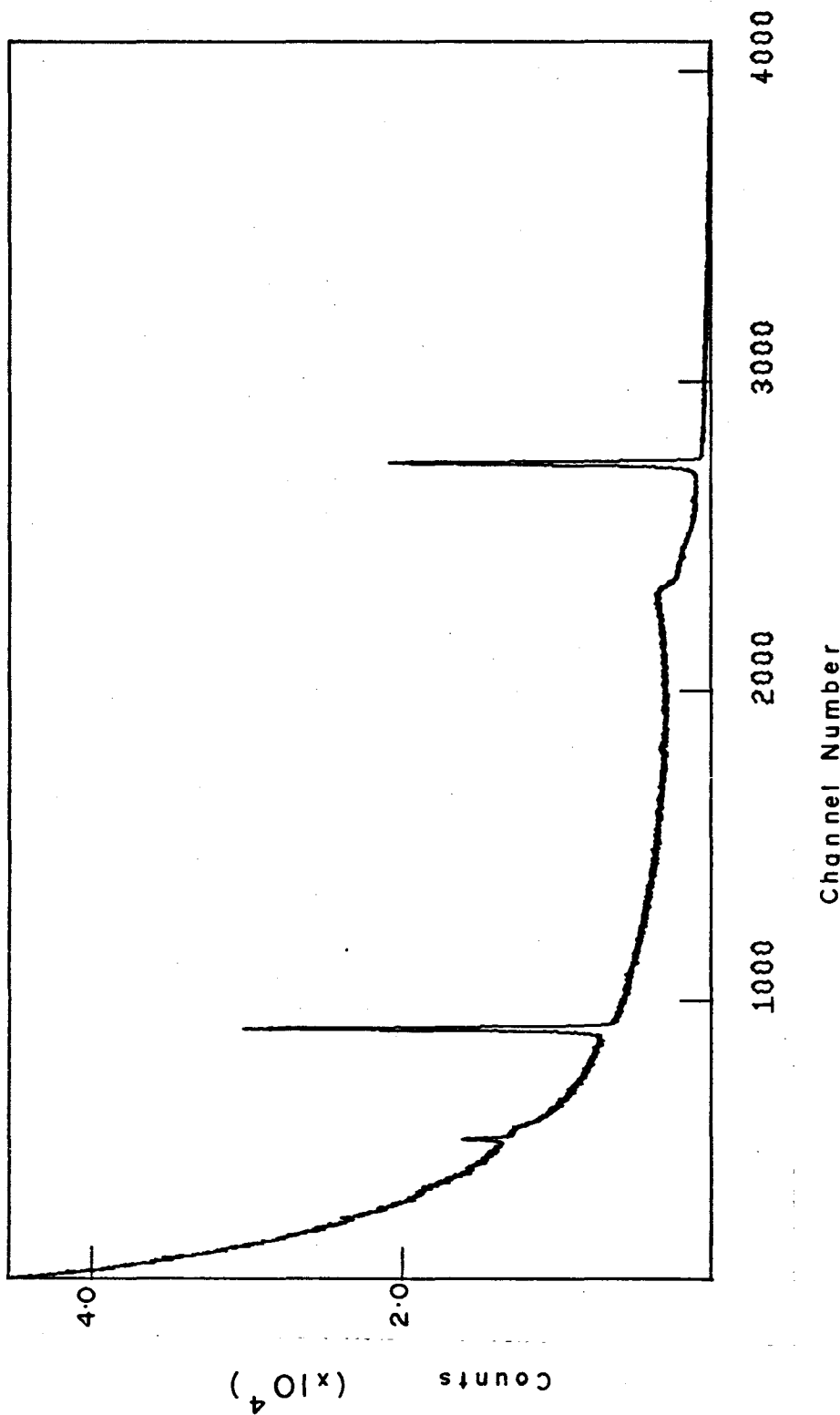


Figure 2.
Copper Potassium Gamma-ray Spectrum

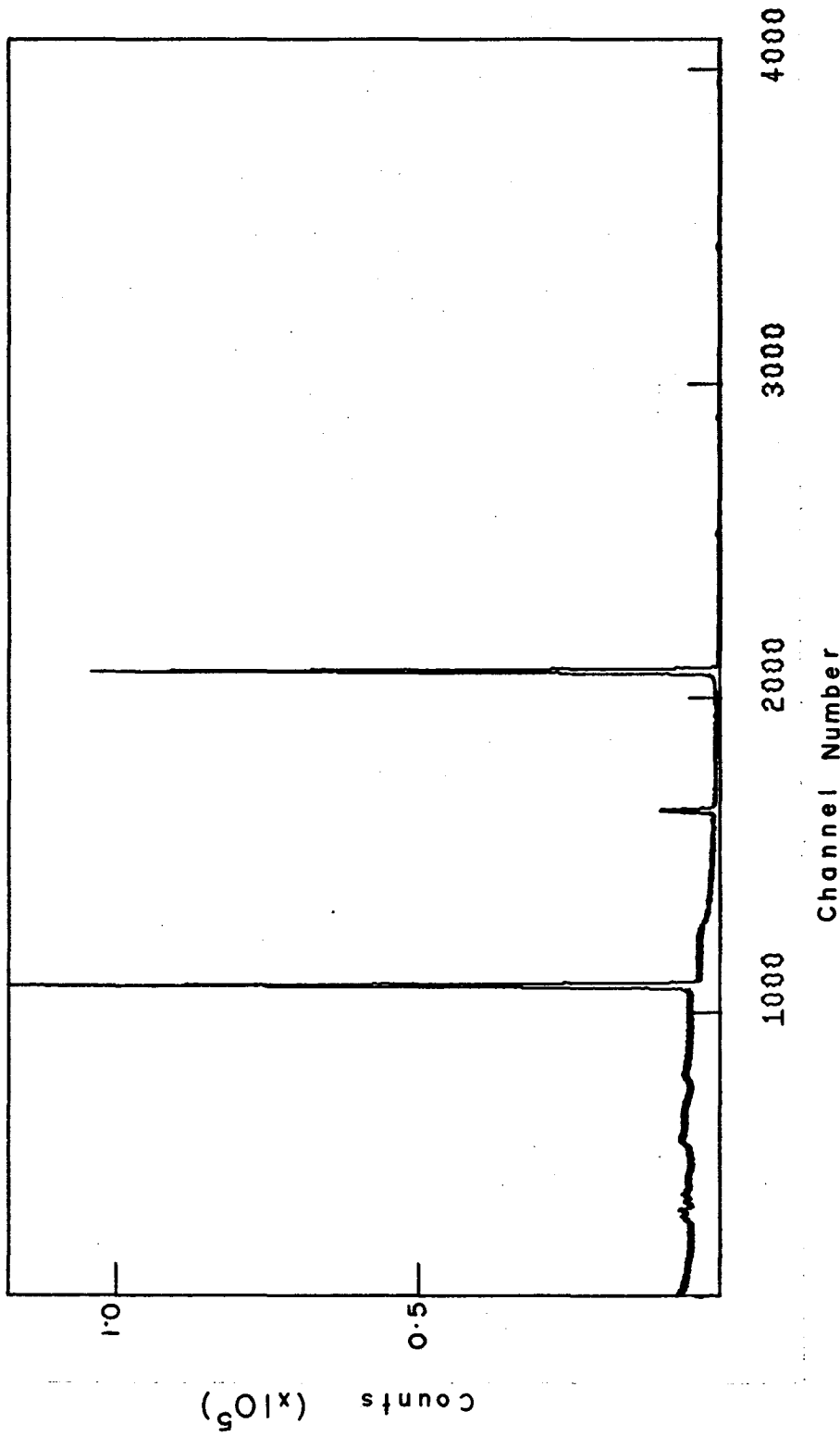


Figure 3.
Ruthenium & Gold Gamma Ray Spectrum

DISCUSSION

The uncertainty present in the results obtained has several sources. Counting experiments are, in general, subject to variations in accordance with counting statistics. The uncertainty from this source for the quantity $\ln \left(\frac{A_1}{A_2} \right)$ can be expressed as:

$$\sigma \left(\ln \left(\frac{A_1}{A_2} \right) \right) = \left[\left(\frac{\sigma(A_1)}{A_1} \right)^2 + \left(\frac{\sigma(A_2)}{A_2} \right)^2 \right]^{\frac{1}{2}}$$

where $\sigma(A_1)$ and $\sigma(A_2)$ are standard deviations due to counting for peak areas A_1 and A_2 . The uncertainty in the half-life calculated from these values is given by

$$\sigma(t_{\frac{1}{2}}) = \frac{(0.693) (\sigma(\lambda_r)^2 + \sigma(\Delta\lambda))^{\frac{1}{2}}}{(\lambda_r - \Delta\lambda)^2}$$

where r indicates a reference isotope, and $\Delta\lambda$ has been defined previously. Derivations for these formulae are given in Appendix D.

Since the peaks found in this work were unusually wide due to the acquisition of large numbers of counts, their boundaries were indistinct. The determination of these boundaries is generally one of the most troublesome problems in peak area measurements and leads to uncertainty in the result.

Substantial gain shifts were observed during most of the measurements. The use of a total-peak-area method of analysis, however, should avoid errors due to this. (Hertogen 74). The same is true for temperature changes, which were present.

When Ge (Li) detectors are used, changes in peak area

with sample position can be dramatic. (Hoste 71 pg. 140)

These changes vary according to energy, and can thus affect peak-area ratios. Although care was taken to avoid variation of source-counter geometry, errors due to this effect cannot be ruled out.

The uncertainty in $\ln \left(\frac{A'}{A_s} \right)$ obtained from standard isotope tests was about 4.5 times that predicted from counting statistics. This illustrates the pitfalls of using these alone. They may be said to represent the case where all instruments and techniques are working perfectly. However, they do present a limit to counting experiments.

Systematic errors must also be avoided. Interfering activities in particular should be guarded against.

During the counting of the copper-potassium sample, potassium-40 was observed as a very weak peak at 1460 Kev. A weak peak was also observed at 1013 Kev. Both of these peaks, however, were sufficiently well resolved to present no problem.

The ruthenium-gold spectra showed peaks which were identified as due to ruthenium-103 and iridium-192. These, too, were well resolved. It is considered that no interfering activities were present in significant quantity. The values found for the half-life of ruthenium-97 show considerable lack of reproducability from run to run. In only two trials did the data not show severe scattering (see figure 4 for examples). These trials were made

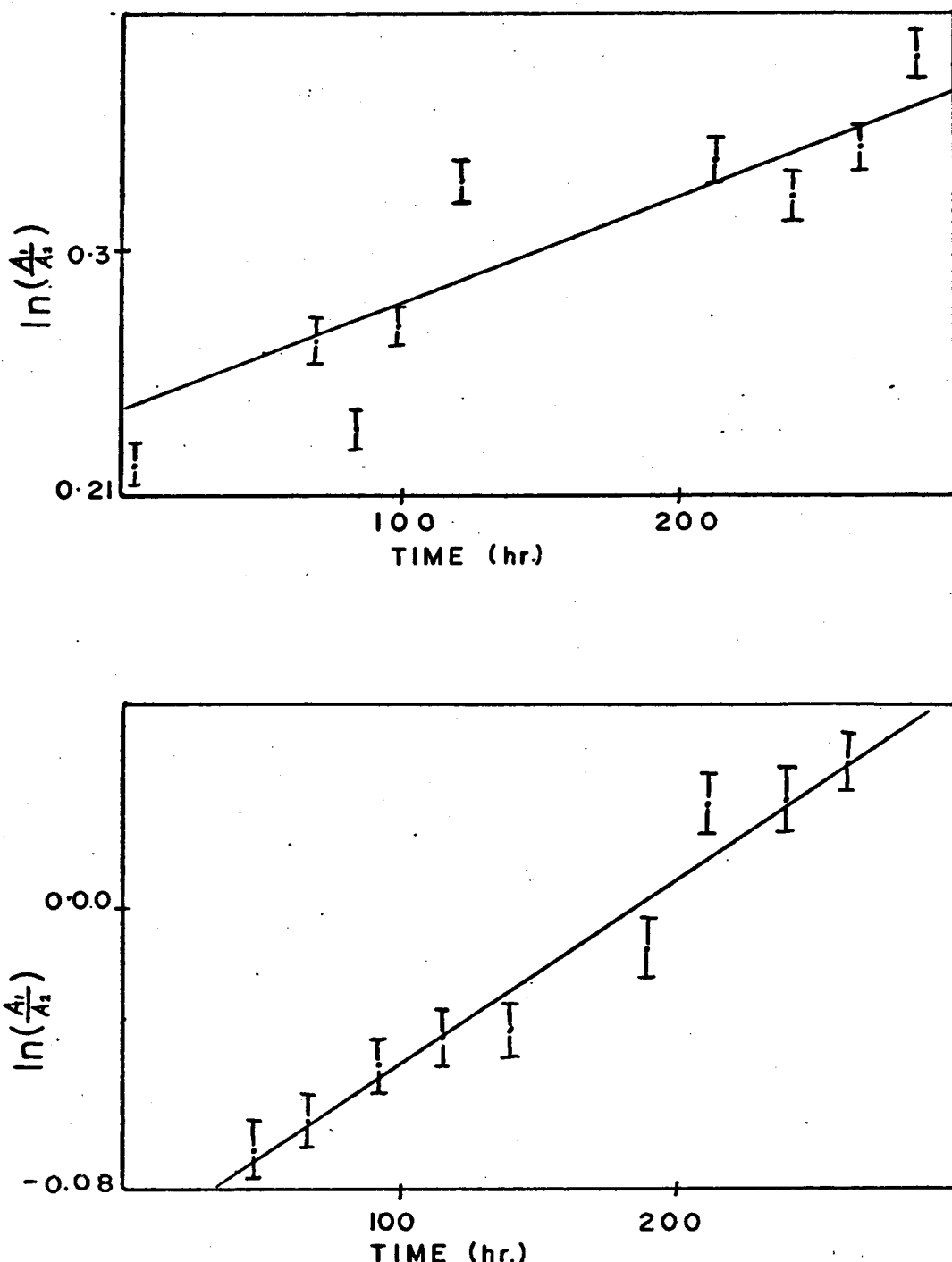


Figure 4.

Ruthenium & Gold: $\ln\left(\frac{A_1}{A_2}\right)$ vs Time

concurrently with the Harshaw detector. The others show evidence of possible instrumental malfunction (the clock channel contents do not follow the count rate, and much intermittent, low energy noise is present). Although it is not clear how peak area ratios may have been affected, it is possible that the lack of reproduceability was due to electronic effects. The two apparently more normal trials do not show the symptoms described above. These observations illustrate the pitfalls of blind faith in instrumentation.

The lack of evidence of any change in half-life caused by change in chemical state is not unexpected if the uncertainties encountered are considered. Where they have been reported, their magnitude has been on the order of a part per thousand (expressed as $\frac{\Delta\lambda}{\lambda}$). This sensitivity has not been achieved in the present work. Theoretical considerations also indicate that any effects present are likely to be very small. The electrons available for chemical manipulation are present in the 4s subshell (Cu) or the 5s and 4d subshells (Ru). These orbitals do not contribute a major portion of the electron density at the nucleus.

The sensitivity achieved in these trials should not be regarded as the ultimate possible using this method of measurement. If the instrumentation employed is well stabilized and its performance is continuously monitored by means of standard sources, considerable improvement may be expected.

A more sophisticated method of peak-area determination could also yield better results. It must be realized, however, that the uncertainty in the half-life of the standard isotope used to give peak area ratios represents a fundamental limit of this method. Results will always be more uncertain than the standard values used inasmuch as only relative quantities are obtained experimentally.

The most useful application of this method is expected to be the questions of identification of activities. It is suitable for identifying the components of a mixture of activities if at least one has been recognized by other means. Qualitative activation analysis is one such undertaking. In many cases, the half-life of an isotope is more characteristic than the energies of its radiations.

CONCLUSION

The decay rate of a radioactive isotope can be determined by measuring its gamma radiation together with that of a reference isotope whose decay rate is known. This measurement can be carried out using a lithium drifted germanium detector. This permits decay rate determination in the presence of other activities if they do not interfere with the radiations selected for study. Corrections for dead time and pulse pile-up are not required. The high sensitivity inherent in this technique clearly reveals even minor malfunctions or limitations of the equipment used. These effects could pass unnoticed when other methods of half-life determination are employed.

APPENDIX A

Electron Capture Decay

The discussion given here is based upon the work of Emery (Emery 72).

The total transition probability for decay by capture of bound electrons can be expressed as:

$$\lambda = \left(\frac{g^2}{2\pi^2} \right) \sum_x n_x C_x f_x$$

where g is the weak interaction coupling constant, n_x is the occupation probability of orbital x , C_x is a shape factor and f_x is given by

$$f_x = \left(\frac{\pi}{2} \right) q_x^2 \beta_x^2 B_x$$

q_x represents the energy of the neutrino emitted when an electron hole is created in orbital x , β_x is the electron wavefunction amplitude for orbital x and B_x is an exchange and overlap factor.

Since the Coulomb field near a nucleus is very strong, the shape of atomic orbitals there is unaffected by external changes. However, the normalization of the wavefunction near the nucleus is affected. The quantities most affected by external changes are therefore n_x and β_x^2 .

In the majority of cases, electron capture involves the $s_{\frac{1}{2}}$ and $p_{\frac{1}{2}}$ orbitals. This leads to the approximation that the quantity C is constant for capture from $s_{\frac{1}{2}}$ and $p_{\frac{1}{2}}$ orbitals, but is zero for other orbitals. The B factors have a weighted value of about one. Therefore the capture

$$\text{rate is approximately } \lambda = \left(\frac{g}{\pi}\right)^2 C \sum_x q_x^2 n_x \beta_x^2 \quad x = s_{\pm}, p_{\pm}$$

This form shows more clearly the effect of changes in chemical parameters such as oxidation state.

APPENDIX B

Optical Spectrum of Ru O₄.py2

The spectrum of Ru O₄.py2 from 320 to 600 m μ is given in figure 5. The maximum at 416 m μ corresponds to that at 420 m μ , reported by Y. Koda (Koda 63). This spectrum, and the correspondence in solubility behaviour between the material prepared and that described in the literature, confirm that Ru O₄.py2 was obtained.

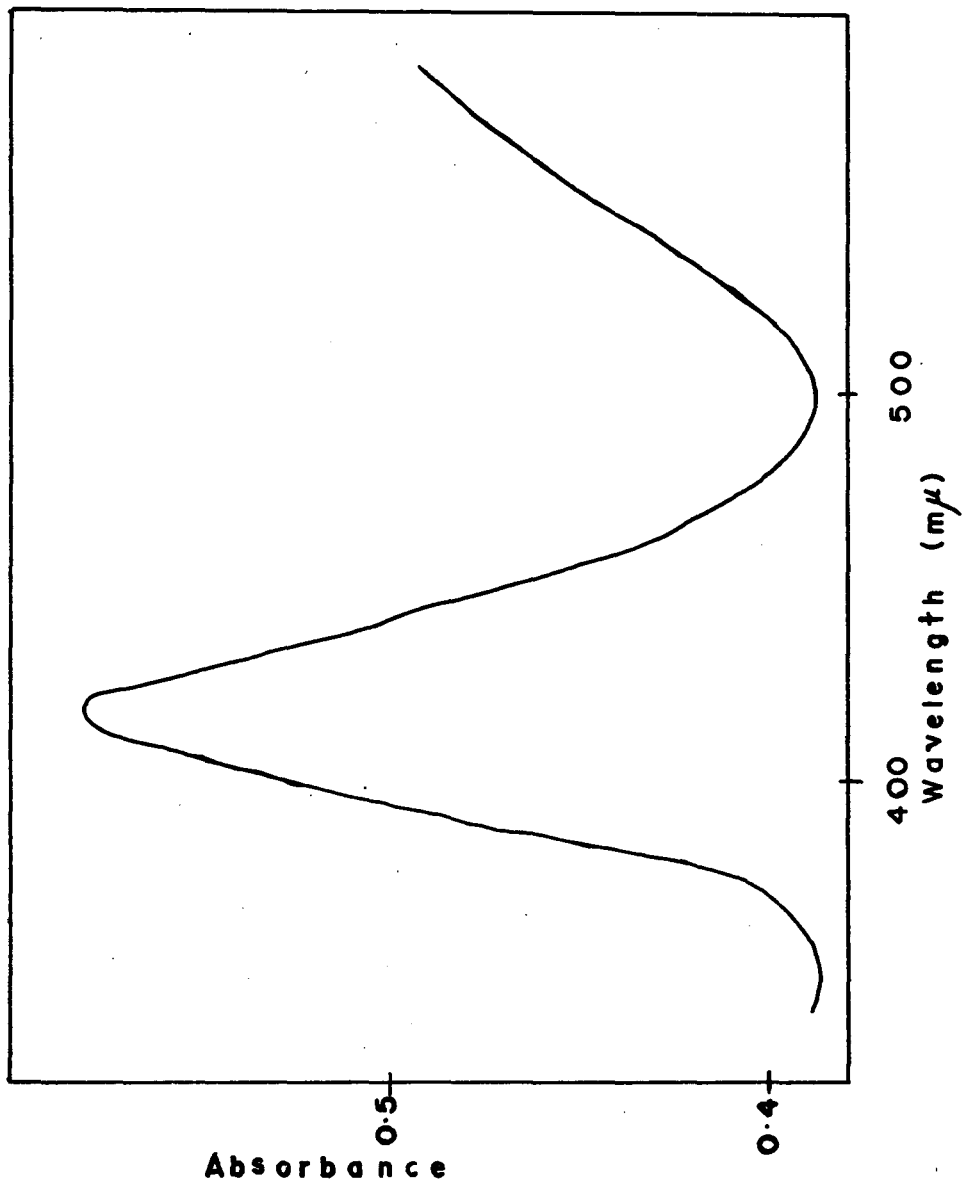


Figure 5.
Optical Spectrum of Ru O₄ · py₂

APPENDIX C

Computer Program For Spectrum Analysis

The program developed for use on the PDP-15 computer was written in the FORTRAN IV and MACRO-15 languages. MACRO-15 is an assembly language, and was used to perform operations not possible in FORTRAN IV. The system used comprised three parts. First, raw data stored on perforated paper tape was read in and checked for "spurious" negative values (vide infra). The region read in could be printed out if desired, and could be compressed by adding together successive groups of four channels. The data were then output, in floating point format, onto paper tape.

The second stage generated a CRT display of the data with six moveable cursor points. Straight lines could be generated between two pairs of these cursors and also displayed. The channel numbers associated with the cursors were outputted on the teletype.

The third stage, using the channel numbers generated by the second step, performed fitting and integration functions and outputted peak areas and standard deviations based on counting statistics. The flowcharts given in figure 6 show the operations involved.

The first program operates as follows; the operator is asked if the data are to be compressed, if so, a flag variable is set to indicate this. A command is requested which will cause the program to begin a new spectrum or continue with the present spectrum.

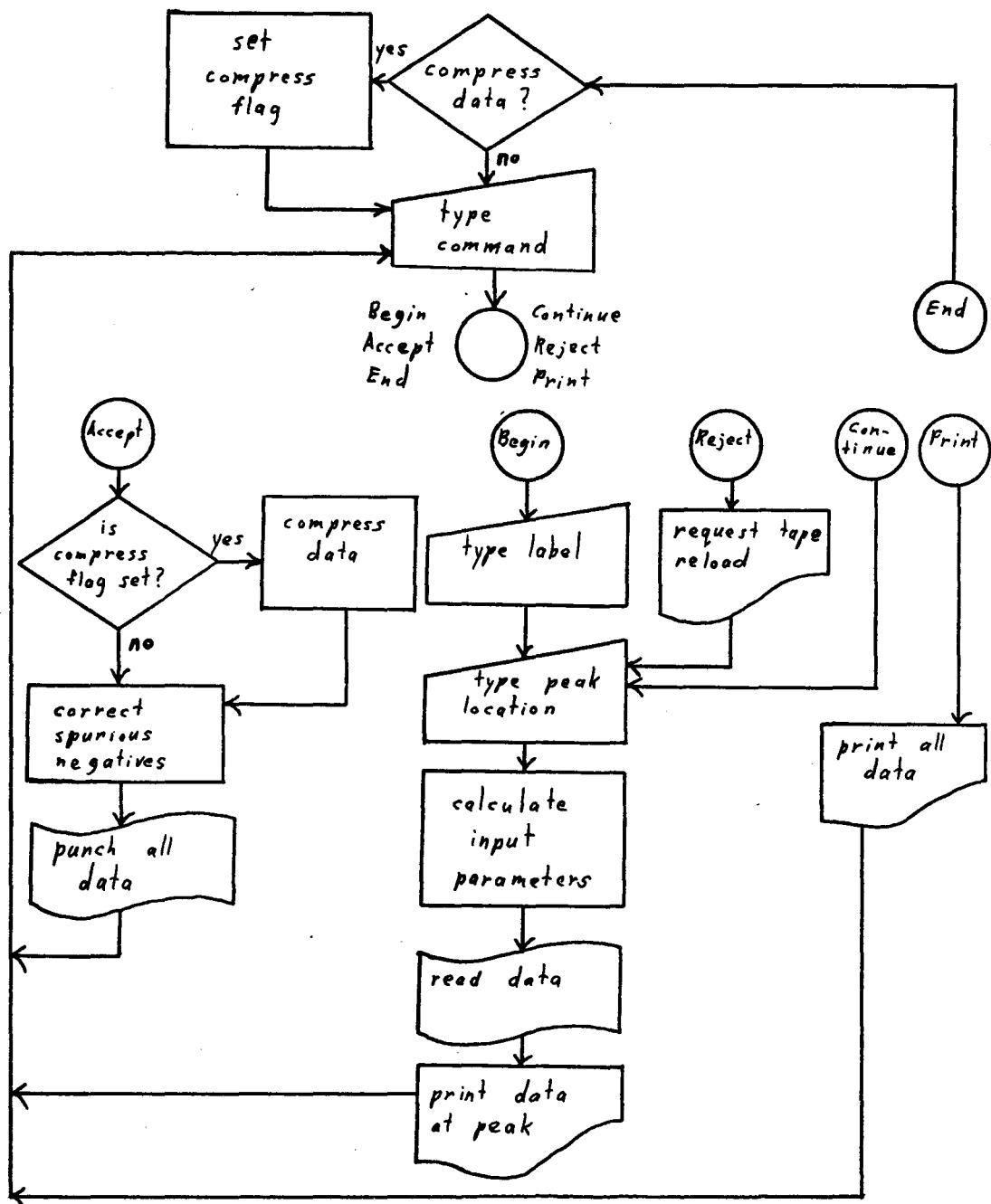


Figure 6a
Flowchart for Program 1.

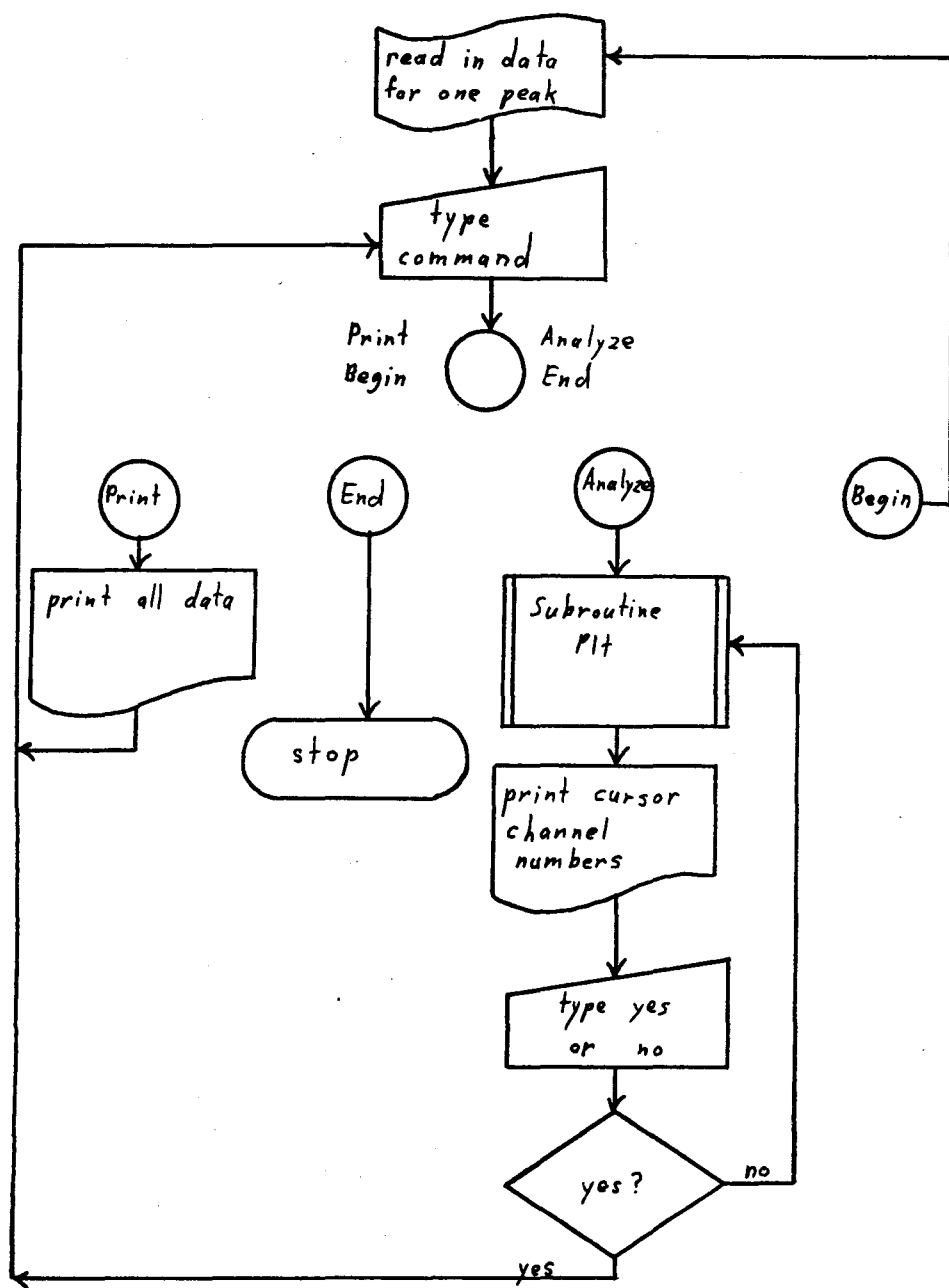


Figure 6b
Flowchart for Program 2.

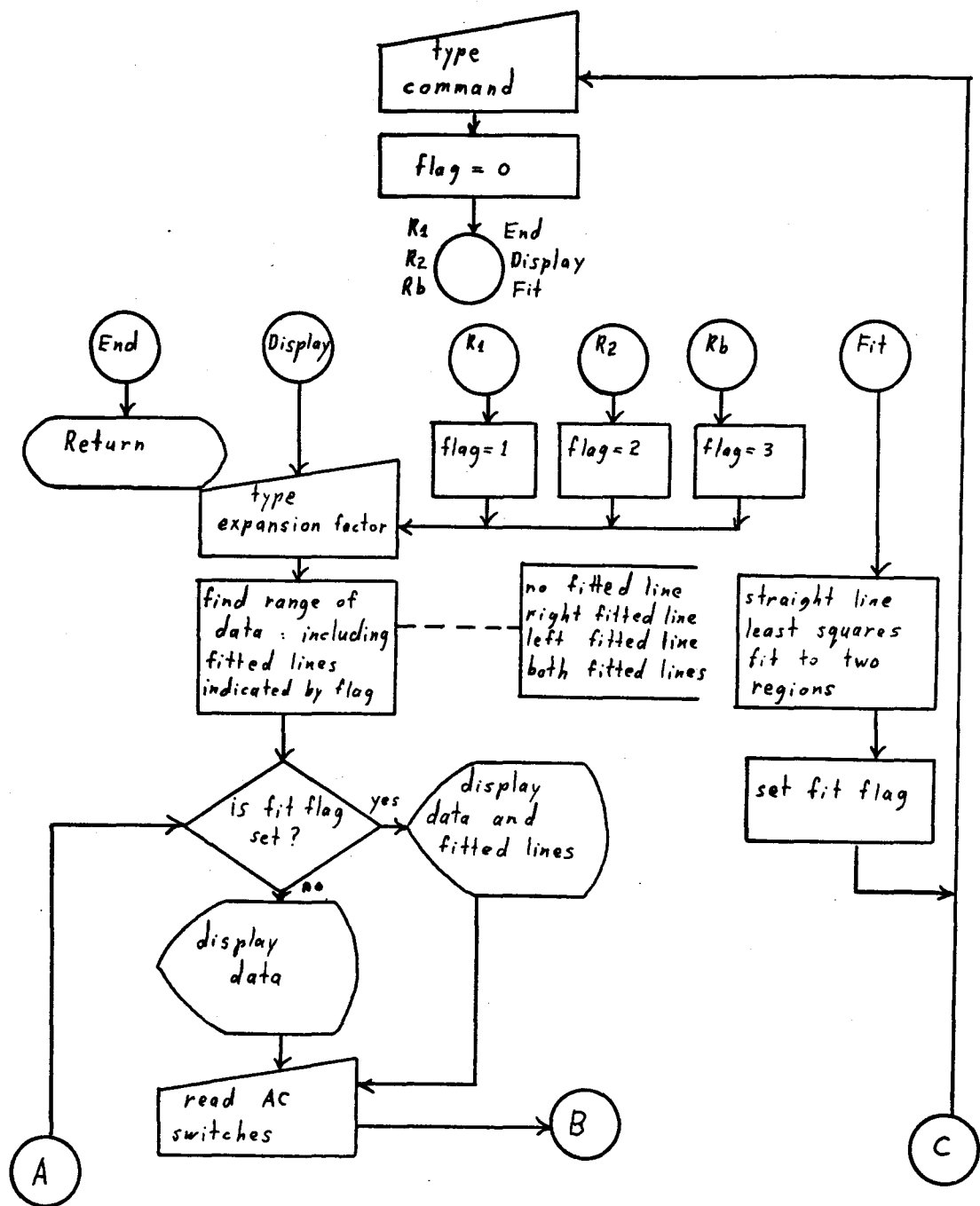


Figure 6c
Flowchart for Subroutine P1t

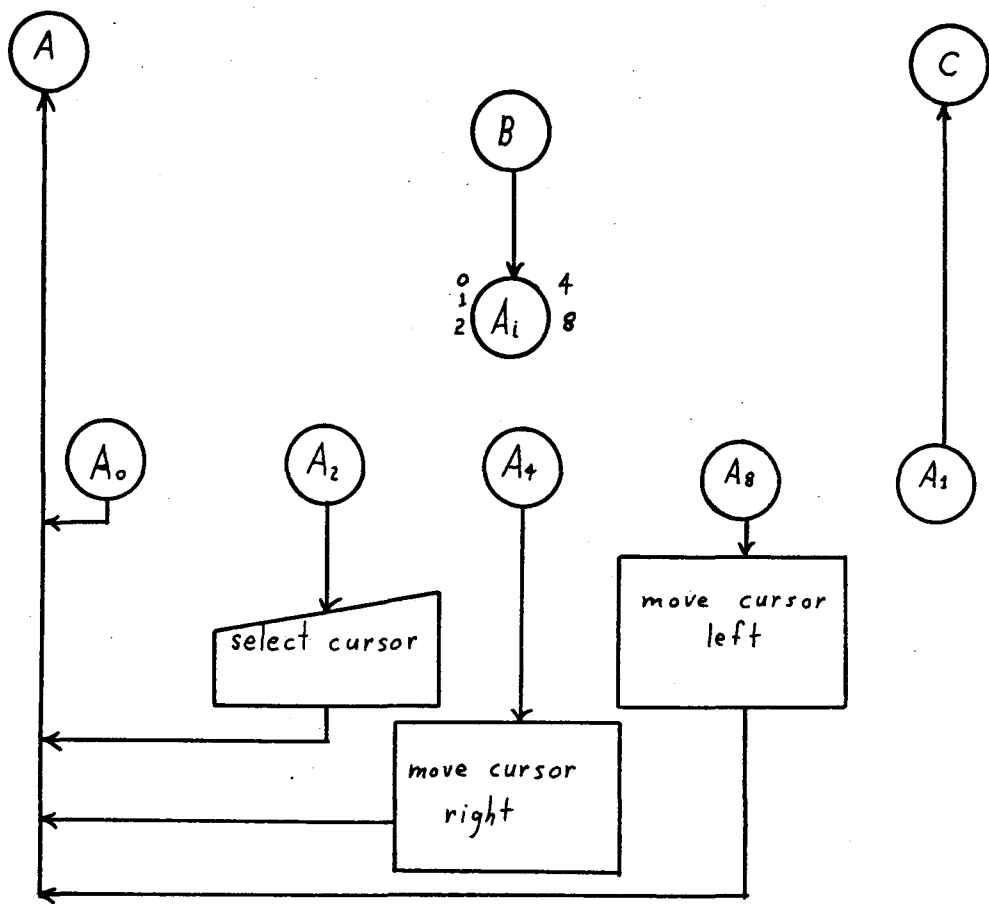


Figure 6d
Flowchart for Subroutine Plt

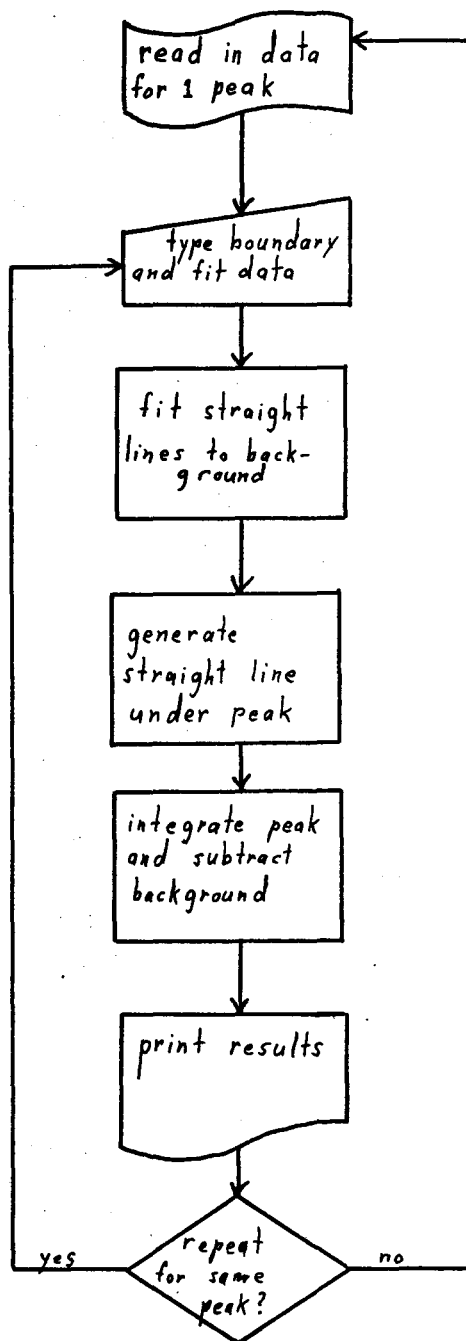


Figure 6e
Flowchart for Program 3.

The next peak location is requested and the required number of channels is calculated and read in. A new command is then required to reject the data or accept it. If accepted, the data are punched in corrected floating point form onto paper tape and the program begins again. If the state of the compression flag is to be changed, a separate command is used.

```
DIMENSION DA(400)
COMMON ND(800)
DATA BEG,CON,ACC,REJ/3HBEG,3HCON,3HACC,3HREJ/
DATA PRI/3HPRI/,END,YES/3HEND,3HYES/
2      WRITE(1,60)
60    FORMAT(1H ,18HTYPE YES FOR COMP.)
      READ(2,61) CM
61    FORMAT(A3)
      ICOM=0
      IF(CM.EQ.YES) ICOM=1
1      WRITE(1,20)
20    FORMAT(1H ,12HTYPE COMMAND)
      READ(2,21) CM
21    FORMAT(A3)
      IF(CM.EQ.BEG) GO TO 50
      IF(CM.EQ.CON) GO TO 51
      IF(CM.EQ.ACC) GO TO 52
      IF(CM.EQ.REJ) GO TO 53
```

IF(CM.EQ.PRI) GO TO 54
IF(CM.EQ.END) GO TO 2
GO TO 1
50 WRITE(1,22)
22 FORMAT(1H ,15HTYPE LABEL(2A3))
READ(2,23) DLL,DL2
23 FORMAT(2A3
NSP=Ø
LOC=Ø
51 WRITE(1,24)
24 FORMAT(1H ,17HTYPE PEAK LOC(I4))
READ(2,25) LOCP
25 FORMAT(I4)
NCH=LOCP+4Ø1-LOC
NSK=NCH-8ØØ+1
LOC=LOCP+4ØØ
CALL RD(ND,NSK,8ØØ)
N1=35Ø
N2=45Ø
GO TO 7Ø
52 NSP=NSP+1
NO=Ø
WRITE(5) DLL,DL2,NSP,ICOM
IF(ICOM.EQ.1) GO TO 62
DO 63 I0=2ØØ,6ØØ
II=I0-2ØØ+1

IF(IL.GT.400) GO TO 63
CALL NEGCH(ND(IO), YJ)
DA(IL)=YJ
63 CONTINUE
WRITE(5) (DA(L), L=1, 400)
GO TO 1
62 DO 10 I=1, 800, 4
NT=I+3
IF(NT.GT.800) GO TO 10
SUM=0
DO 11 J=I, NT
CALL NEGCH(ND(J), YJ)
SUM=SUM+YJ
11 CONTINUE
NO=NO+1
DA(NO)=SUM
10 CONTINUE
WRITE(5) (DA(L), L=1, 200)
GO TO 1
53 WRITE(1, 26)
26 FORMAT(1H , 11HRELOAD TAPE)
LOC=0
GO TO 51
54 N1=1
N2=800
70 DO 40 IP=N1, N2, 5

```
IF( IP.EQ.400) WRITE(1,71)

71  FORMAT(1H )

      NTO=IP+4

      WRITE (1,41) (ND(L),L=IP,NTO)

41  FORMAT(1H ,5I8)

40  CONTINUE

      GO TO 1

      STOP

      END
```

The subroutine RD reads in the number of channels specified by the variable NIN, first skipping the number of channels given by NSK. The contents of the channels are placed in the array indicated by ND.

```
.TITLE RD
.GLOBL RD,.DA
RD      .
JMS* .DA
JMP .+3=1
ND      .DSA .
NSK     .DSA .
NIN     .DSA .
LAC* NIN
TCA
DAC INCOUN
LAC* ND
DAC ST
LAC* NSK
TCA
DAC COUNT
LAC (1
DAC FL
LAC* NSK
SNA
JMP LST
```

PRD JMS READ
CLL
SNA
JMP PRD
AND (77
RTL
RAL
SWHA
DAC DATUM
JMS READ
CLL
AND (77
SWHA
RTR
RAR
XOR DATUM
DAC DATUM
JMS READ
CLL
AND (77
XOR DATUM
DAC DATUM
LAC FL
SZA
JMP SKIP
LAC DATUM

DAC* ST
ISZ ST
SKIP ISZ COUNT
JMP PRD
JMP LST
READ Ø
IOF
RSA
RSF
JMP .-1
RRB
ION
JMP* READ
LST LAC FL
SNA
JMP* RD
LAC (Ø
DAC FL
LAC INCOUN
DAC COUNT
JMP PRD
RSA = 700104
RSF = 700101
RRB = 700112
ION = 700042
IOF = 700002

```
INCOUN .DSA 0
FL     .DSA 0
COUNT  .DSA 0
DATUM  .DSA 0
ST     .DSA 0
.END
```

Occasionally, a number will be obtained from the multi-channel analyser which is sufficiently large to set the "sign bit" of the computer. These numbers appear as "spurious negatives". The subroutine NEGCH uses subroutine CONEG to convert these to floating point numbers of the correct value.

```
SUBROUTINE NEGCH (N,YJ)
IF(N.EQ.0) GO TO 50
IF(N.GT.0) GO TO 51
CALL CONEG (N,NR1,NR2)
YJ=FLOAT(NR1) + FLOAT(NR2)+32768.0
WRITE (1,20) N,YJ
20   FORMAT(2H ,17H NEGATIVE CONVERTED,4X,1I0 ,4X, F15.2)
      GO TO 100
50   YJ=0.0
      WRITE(1,21)
21   FORMAT(2H ,9HDATA PT=0)
      GO TO 100
51   YJ=FLOAT(N)
```

100 RETURN

END

.TITLE CONEG

.GLOBL CONEG, 1DA

CONEG Ø

JMS* .DA

JMP .+3+2

N .DSA Ø

NRL .DSA Ø

NR2 .DSA Ø

LAC* N

AND (77777

DAC* NRL

LAC* N

AND (7000000

SWHA

RTR

RTR

RTR

RAR

DAC* NR2

JMP* CONEG

END

The second program is used to establish peak parameters. The data for a peak is read in, then a command is requested which can stop the program, cause another peak to be read in, print the data, or transfer to the display routine. Upon return from the display program, the locations of the cursors are printed, and the program can be caused to return to the display program, or to ask for a command.

```
REAL IYS,IAN,IEN,ICM,ICN  
DIMENSION NB(6)  
COMMON DA(400),ICOM  
DATA IYS,IAN,IEN/3HYES,3HANA,3HEN/  
DATA BEG/3HBEG/,PRI/3HPRI/  
PAUSE 1  
53 READ(3) DLA1,DLA2,NSP,ICOM  
      N2=400  
      IF(ICOM.EQ.1) N2=200  
      READ(3) DA(L),L=1,N2)  
      WRITE(1,24) DLA1,DLA2,NSP  
24   FORMAT(1H ,8HSPECTRUM,2X,2A3,2X,4HPEAK,2X,I4)  
1    WRITE(1,20)  
20   FORMAT(1H ,16HTYPE COMMAND(A3))  
      READ(2,21) ICM  
21   FORMAT(A3)  
      IF(ICM.EQ.IAN) GO TO 51  
      IF(ICM.EQ.IEN) GO TO 52
```

IF(ICM.EQ.BEG) GO TO 53
IF(ICM.EQ.PRI) GO TO 54
GO TO 1

51 DO 240 I=1,6
NB(I)=I

240 CONTINUE

241 CALL PLT(NB)
WRITE(1,22) (NB(L),L=1,6)

22 FORMAT(1H ,6I8)
WRITE(1,70)
FORMAT(1H ,44HTYPE YES FOR CONTINUE, NO FOR NEW BOUNDS
(A3))
READ(2,21) ICN
IF(ICN.NE.IYS) GO TO 241
WRITE(1,25) DLA1,DLA2,NSP,(NB(L),L=1,6)

25 FORMAT(1H ,2A3,4X,14/1H ,6I8)
GO TO 1

54 NT=400
IF(ICOM.EQ.1) NT=200
DO 10 IO=1,NT,5
INT=IO+4
WRITE(1,55) IO,(DA(L),L=IO,INT)
55 FORMAT(1H ,I4,2X,5F10.1)
100 IX=0
CALL SW(IX)
IF(IX.EQ.1) GO TO 1
IF(IX.NE.0) GO TO 100

10 CONTINUE

GO TO 1

52 STOP

END

Subroutine Plt performs the display functions. It is used as follows. A command is requested which results in return to the main program, display of the data and cursors on an oscilloscope, fitting of straight lines to the data between the first and second, and fifth and sixth cursors, or inclusion of various portions of these lines in the range finding operation. Once the straight lines have been fitted, they too are displayed.

After a display has been initiated, the first four AC switches can be used to select a cursor, move the current cursor forwards or backwards, or end the display and call for a command.

SUBROUTINE PLT(NB)

REAL MAX,MIN, ID

DIMENSION NB(6), ILP(400), ISP(400)

COMMON DA(400), ICOM

DATA END,REP,FIT/3HEND,3HREP,3HFIT/

DATA RS1,RS2,RSB/3HRS1,3HRS2,3HRSB/

FVFIT(S,Y,IP)=FLOAT(IP)*S+Y

FCONV(V)=(V-MIN)*CONV

NDEL=0
N1=1
N2=400
IF(ICOM.EQ.1) N2=200
IF IT=0
S1=1.0
S2=1.0
YI1=1.0
YI2=1.0
GO TO 90
52 WRITE(1,60)
60 FORMAT(1H ,21HTYPE EXP FACTOR(F6.2)/1H ,3X,1H.)
READ(2,61) ID
61 FORMAT(F6.2)
MAX=0.0
MIN=DA(N1)
DO 10 I=N1,N2
IF(DA(I).GT.MAX) MAX=DA(I)
IF(DA(I).LT.MIN) MIN=DA(I)
IF((IR.NE.1).AND.(IR.NE.3)) GO TO 1
VT=FVFIT(S1,YI1,I)
IF(VT.LT.MIN) MIN=VT
1 IF((IR.NE.2).AND.(IR.NE.3)) GO TO 10
VT=FVFIT(S2,YI2,I)
IF(VT.LT.MIN) MIN=VT
10 CONTINUE

CONV=(495.0/(MAX-MIN))*ID
NCO=1
NXM=10
IF(ICOM.EQ.1) NXM=20
IF((IR.EQ.1).OR.(IR.EQ.2)) NXM=20
DO 200 IPL=N1,N2
ISP(IPL)=FCONV(DA(IPL))
ISP(IPL)=ILIM(ISP(IPL))
IF(IFIT.NE.1) GO TO 200
IF(IPL.LE.200) XPL=FVFIT(S1,YI1,IPL)
IF(IPL.GT.200) XPL=FVFIT(S2,YI2,IPL)
ILP(IPL)=FCONV(XPL)
ILP(IPL)=ILIM(ILP(IPL))
200 CONTINUE
204 CALL DISPA(ISP,NXM,N1,N2)
IF(FIT.NE.1) GO TO 202
CALL DISPA(ILP,NXM,N1,N2)
CALL DISPA(ISP,NXM,N1,N2)
202 DO 203 IPL=1,6
IF((NB(IPL).GT.N2).OR.(NB(IPL).LT.N1)) GO TO 203
IX=NB(IPL)*NXM
IV=NB(IPL)
IY=ISP(IV)
CALL DISP(IY,IX)
CALL DISP(IY,IX)
203 CONTINUE

NDEL=NDEL+1
IF(NDEL.LT.10)GO TO 204
NDEL=0
IDZ=0
CALL SW(IDZ)
IF(IDZ.NE.0) GO TO 224
GO TO 204
224 IF(IDZ.EQ.1) GO TO 90
IF(IDZ.NE.2) GO TO 208
WRITE(1,209)
209 FORMAT(1H ,19HTYPE CURSOR NO.(I3))
READ(2,210) NCO
210 FORMAT(I3)
GO TO 204
208 IF(IDZ.EQ.4) NADV=+1
IF(IDZ.EQ.8) NADV-1
NB(NCO)=NB(NCO)+NADV
IF(NB(NCO).GT.N2) NB(NCO)=N2
IF(NB(NCO).LT.N1) NB(NCO)=N1
GO TO 204
90 WRITE(1,22)
22 FORMAT(1H ,11HTYPE COMMAND)
READ(2,23) CM
23 FORMAT(A3)
IR=0
IF(CM.EQ.END) GO TO 50

IF(CH.EQ.REP) GO TO 100
IF(CM.EQ.FIT) GO TO 53
IF(CM.EQ.RS1) IR=1
IF(CM.EQ.RS2) IR=2
IF(CM.EQ.RSB) IR=3
IF(IR.NE.0) GO TO 56
GO TO 90

100 N1=1
N2=400
GO TO 52

56 IF(IR.NE.1) GO TO 57
N1=1
N2=200
IF(IR.NE.2) GO TO 52

57 N1=201
N2=400
GO TO 52

53 CALL FIT2(NB(1),NB(2),S1,YI1)
CALL FIT2(NB(5),NB(6),S2YI2)
IF IT=1
GO TO 90

50 RETURN
END

Subroutine DISP plots one data point on the display.

Subroutine DISPA displays an array on the oscilloscope.

```
.TITLE DISP  
.GLOBL DISP,.DA  
  
DISP    $  
        JMS* .DA  
        JMP   .+2+2  
  
IY      .DSA  $  
IX      .DSA  $  
        LAC*  IY  
        RTL  
        RTL  
        RTL  
        DACY  
        LAC*  IX  
        RTL  
        RTL  
        RTL  
        DACX  
        JMP*  DISP  
DACY= 701524  
DACX= 701544  
.END
```

.TITLE DISPA
.GLOBL DISPA, .DA

DISPA \$
JMS* .DA
JMP .+4+1
IAR .DSA \$
NX .DSA \$
N1 .DSA \$
N2 .DSA \$
LAC* NX
DAC IX
LAC* IAR
TAD* N1
TAD (-1
DAC LOCL
LAC* N2
TCA
TAD* N1
DAC NCOUN
SHOW LAC* LOCL
RTL
RTL
RTL
DACY
LAC IX
RTL

```
RTL  
RTL  
DACX  
ISZ    LOC1  
LAC    IX  
TAD*   NX  
DAC    IX  
ISF    NCOUN  
JMP    SHOW  
JMP*   DISPA  
DACY=  701524  
DAXC=  701544  
IX     .DSA  $  
LOC1  .DSA  $  
NCOUN .DSA  $  
.END
```

In subroutine DISP , IY is the Y coordinate and IX is the x coordinate. In subroutine DISPA , IAR indicates the array, NX the horizontal increment size, N1 the first element of the array to be plotted and N2 the last element to be plotted.

Subroutine SW reads the AC switches.

```
.TITLE  SW  
.GLOBL  SW, .DA  
SW    $
```

```

JMS*      .DA
JMP      .+2+2
IDZ      .DSA      0
LAS
AND      (17
DAC*      IDZ
JMP*      SW
.END

```

Subroutine ILIM ensures that values to be plotted
are within preset limits.

```

FUNCTION    ILIM ( IA )
IT=IA
IF ( IA.GT.4095) IT = 4095
IF ( IA.LT.2     ) IT = 2
ILIM = IT
RETURN
END

```

Subroutine FIT2 performs the fitting operation.

```

SUBROUTINE FIT2(N1,N2,XM,Xc)
COMMON DA(400),NPOS
SUM1=0.
SUM2=0.
SUM3=0.

```

```
SUM4=0  
DO 10 J=N1,N2  
YJ=DA(J)  
X=J  
SUM1=SUM1+1.0/YJ  
SUM2=SUM2=(X*X)/YJ  
SUM3=SUM3+(X)/YJ  
SUM4=SUM4+X  
CONTINUE  
H1=SUM1  
H2=SUM2  
H3=SUM3  
XN=N2-N1+1  
XNUM=SUM1*SUM4-XN*SUM3  
YNUM=XN*SUM2-SUM4*SUM3  
XDEN=SUM1*SUM2-SUM3*SUM3  
XM=YNUM/XDEN  
XC=YNUM/XDEN  
RETURN  
END
```

The final step in the analysis is shown below. The data for a peak is read in and a request is made for the information obtained in step two. A straight line is then fitted to the indicated sections of background. The value and statistical uncertainty of each line is determined at the

appropriate peak boundary. A third line is generated between the peak boundaries using this information. Finally, the peak area and its statistical uncertainty are calculated by summing the contents of the channels between the peak boundaries minus their associated background contributions. The result is then printed.

```
COMMON DA(400),NPOS
DATA YES/3HYES/
1 PAUSE 1
READ(3) DLA1,DLA2,NPKS,ICOM
N2=400
IF(ICOM.EQ.1) N2=200
READ(3) ((DA(L),L=1,N2)
WRITE(1,20) DLA1,DLA2,NPKS
20 FORMAT(1H ,8HSPECTRUM,4X,2A3,4X,8HPEAK NO.,I6)
94 WRITE(1,21)
21 FORMAT(1H ,20HTYPE PARAMETERS(6I4))
READ(2,22) NL1,NL2,NL3,NU1,NU2,NU3
22 FORMAT(6I4)
NDIL=NL2-NL1
NDIU=NU3-NU2
ML2=NL3+1
MUL=NUL-1
YNL1=DA(NL1)
YNL2=DA(NL2)
YNU1=DA(NU2)
```

```
YNU2=DA(NU3)

IF(NL1.EQ.NL2) BL=YNL2

IF(NU2.EQ.NU3) BR=YNU1

IF(NDIL.EQ.1) BL=(YNL1+YNL2)/2.0

IF(NDIU.EQ.1) BR=(YNU1+YNU2)/2.0

IF(NDIL.LT.2) GO TO 11

NPOS=NL3

CALL FIT(NL1,NL2,BL,H1,H2,H3,XNL2,XDENL,XML,XCL)

11 IF(NDIU.LT.2) GO TO 13

NPOS=NUL

CALL FIT(NU2,NU3,BR,F1,F2,F3,XNU1,XDENU,XMU,XCU)

13 XDEN=NUL-NL3

IF(NDIL.EQ.1) XDEN=XDEN+0.5

IF(NDIU.EQ.1) XDEN=XDEN+0.5

XM=(BR-BL)/XDEN

IF(NDIL.EQ.1) BL=BL+0.5*XM

IF(NDIU.EQ.1) BR=BR-0.5*XM

IF(NL1.EQ.NL2) SBL=BL

IF(NU2.EQ.NU3) SBR=BR

IF(NDIL.EQ.1) SBL=(BL*BL)/(YNL2+YNL1)

IF(NDIU.EQ.1) SBR=(BR*BR)/(YNU2+YNU1)

IF(NDIL.LT.2) GO TO 15

NPOS=NL3

CALL ERR(NL1,NL2,XML,XCL,XNL2,H2,H3,XDENL,SBL)

15 IF(NDIU.LT.2) GO TO 17

NPOS=NUL
```

```

CALL ERR(NU2,NU3,XMU,XCU,XNUL,F1,F2,F3,XDENU,SBR)

17 A=Ø.

SA=Ø

WRITE(1,9Ø) BR,SBR,BL,SBL

9Ø FORMAT(1H ,5Hr..PT,F15.2,5H..ERR,F15.2/1H ,1HL,
          F15.2,F15.2)
AT=Ø

BCK=Ø

SBCK=Ø

XNL2=NL3

XNUL=NUL

DN=XNUL-XNL2

ZM=(BR-BL)/DN

SM=(SBR+SBL)/(DN*DN)

SC=(SBR*XNL2*XNL2+SBL*XNUL*XNUL)/(DN*DN)

SMC=-(XNL2*SBR+XNUL*SBL)/(DN*DN)

DO 19 J=ML2,MU1

YJ=DA(J)

X=J

A=A+YJ-(ZM*X+C)

BCK=BCK+ZM*X+C

SBCK=SBCK+SM*X*X+SC+2.Ø*SMC*X

AT=AT+YJ

SA=SA+YJ+(SM*X*X+SC+2.Ø*SMC*X)

19 CONTINUE

SA=SQRT(SA)

SBCK=SQRT(SBCK)

```

```

      WRITE(1,72) A,SA
72   FORMAT(1H ,SHAREA=,F15.2/1H ,10HSTD. DEV.=,F15.2)
      WRITE(1,91) AT,BCK,SBCK
91   FORMAT(1H ,10HTOTAL AREA,F15.2/1H ,3HBCK,F15.2,4HSBCK,
              F15.2)
      WRITE(1,92)
92   FORMAT(1H ,18HTYPE YES TO REPEAT)
      READ(2,93) CM
93   FORMAT(A3)
      IF(CM.EQ.YES) GO TO 94
      GO TO 1
      STOP
      END

```

Subroutine FIT fits the data between two channels to a straight line by a least-squares procedure. The value of the line at a predetermined channel is also calculated. Subroutine ERR calculates the variance of the value found by subroutine FIT.

```

SUBROUTINE FIT(N1,N2,B,H1,H2,H3,XN,XDEN,XM,XC)
COMMON DA(400),NPOS
SUM1=0
SUM2=0
SUM3=0
SUM4=0
DO 10 J=N1,N2
YJ=DA(J)

```

```

X=J

SUM1+SUM1+1.0/YJ

SUM2=SUM2+(X*X)/YJ

SUM3=SUM3+(X)/YJ

SUM4+SUM4+X

10 CONTINUE

H1+SUM1

H2=SUM2

H3=SUM3

XN=N2-N1+1

XNUM=SUM1*SUM4-XN*SUM3

YNUM=XN*SUM2-SUM4*SUM3

XDEN=SUM1*SUM2-SUM3*SUM3

XM=XNUM?XDEN

XC=YNUM/XDEN

TXN=NPOS

B=XM*TXN+XC

RETURN

END

SUBROUTINE ERR(N1,N2,XM,XC,XN,H1,H2,H3,XDEN,SB)
COMMON DA(400),NPOS
S=0
DO 16 J=N1,N2
YJ =DA(J)
X=J

```

```
ST=XM*X+XC-YJ  
S=S+(ST*ST)/YJ  
16 CONTINUE  
S=S/(XN-2.0)  
SM=S*H1/XDEN  
SC=S*H2/XDEN  
SMC=-S*H3/XDEN  
TXN=NPOS  
SB=TXN*TXN*SM+SC+2.0*TXN*SMC  
RETURN  
END
```

It has been found that the ability to display a fit to the background with the data is very useful. This is especially useful where the background slopes steeply.

More extensive use of the MACRO-15 language, and the use of magnetic data storage devices could allow this system to be written as a single program. This would greatly facilitate the analysis and would help in choosing peak parameters, since areas would be instantly available for trial sets of boundaries.

APPENDIX D

Derivation of Uncertainty Formulae

The uncertainty of the quantity $\ln(A_1/A_2)$ can be

→ found as is shown below using the propagation of errors technique.

For peak areas A_1 and A_2 having standard deviations $\sigma(A_1)$ and $\sigma(A_2)$, the standard deviation of the ratio A_1/A_2 → is given by the usual propagation of error calculations (Bevington 68) as

$$\sigma\left(\frac{A_1}{A_2}\right)^2 = \left(\frac{A_1}{A_2}\right)^2 \left[\left(\frac{\sigma(A_1)}{A_1}\right)^2 + \left(\frac{\sigma(A_2)}{A_2}\right)^2 \right]$$

assuming that A_1 and A_2 are independent of one another.

The standard deviation of $\ln(A_1/A_2)$ is then obtained.

$$\sigma\left(\ln\left(\frac{A_1}{A_2}\right)\right)^2 = \frac{\left(\frac{\sigma(A_1)}{A_1}\right)^2}{\left(\frac{A_1}{A_2}\right)^2}$$

That is

$$\sigma\left(\ln\left(\frac{A_1}{A_2}\right)\right)^2 = \left(\frac{A_1}{A_2}\right)^2 \left(\frac{A_1}{A_2}\right)^2 \left[\left(\frac{\sigma(A_1)}{A_1}\right)^2 + \left(\frac{\sigma(A_2)}{A_2}\right)^2 \right]$$

and $\sigma\left(\ln\left(\frac{A_1}{A_2}\right)\right) = \left[\left(\frac{\sigma(A_1)}{A_1}\right)^2 + \left(\frac{\sigma(A_2)}{A_2}\right)^2 \right]^{\frac{1}{2}}$

The uncertainty of the half-life calculated by

$$t_{1/2} = \frac{0.693}{\lambda_r - \Delta\lambda}$$

is obtained by a similar process.

$$\sigma(t_{\frac{1}{2}})^2 = \left(t_{\frac{1}{2}}\right)^2 \left[\left(\frac{\sigma(\lambda_r - \Delta\lambda)}{(\lambda_r - \Delta\lambda)^2} \right)^2 + 0 \right]$$

$$\sigma(t_{\frac{1}{2}})^2 = \frac{\left(t_{\frac{1}{2}}\right)^2}{(\lambda_r - \Delta\lambda)^4} \left(\sigma(\lambda_r)^2 + \sigma(\Delta\lambda)^2 \right)$$

that is,

$$\sigma(t_{\frac{1}{2}}) = \frac{\left(t_{\frac{1}{2}}\right) \left(\sigma(\lambda_r)^2 + \sigma(\Delta\lambda)^2 \right)^{\frac{1}{2}}}{(\lambda_r - \Delta\lambda)^2}$$

BIBLIOGRAPHY

Anders 69

O.U. Anders
Nucl. Inst. & Meth. 68 205 (1969)

Bainbridge 53

K.T. Bainbridge et al
Phys. Rev. 90 430 (1953)

Bevington 68

P.R. Bevington
Data Reduction and Error Analysis for the
Physical Sciences
McGraw-Hill N.Y. 1968

Cabell 70

M.J. Cabell and M. Wilkins
J. Inorg. Nucl. Chem. 32 1409 (1970)

Emery 72

G.T. Emery
Ann. Rev. Nucl. 22 165 (1972)

Gagneux 70

von St. Gagneux et al
Helv. Phys. Acta 43 39 (1970)

Hertogen 74

J. Hertogen et al
Nucl. Inst. & Meth. 115 197 (1974)

Hoste 71

J. Hoste et al
Activation Analysis
C.R.C. Press, Cleveland, Ohio 1971

Katcoff 58

S. Katcoff
Phys. Rev. 111 575 (1958)

Koda 63

Y. Koda
Inorg. Chem. 2 1306 (1963)

Lederer 67

C.M. Lederer et al

Table of Isotopes 6th ed
John Wiley & Sons, N.Y. 1967

Merritt 62

Merritt and Taylor
Can. J. Phys. 40 1044 (1962)

Ruff 24

O.R. Ruff and E. Vidic
Z. Anorg. Allg. Chem. 136 49 (1924)

Wyatt 72

E.I. Wyatt et al
Nucl. Sci. Eng. 48 319 (1972)